Boundary-condition-varying circle billiards and gratings: the Dirichlet singularity

2008 J. Phys. A: Math. Theor. 41 135203

(http://iopscience.iop.org/1751-8121/41/13/135203)

IOP PUBLISHING JOURNAL OF PHYSICS A: MATHEMATICAL AND THEORETICAL

J. Phys. A: Math. Theor. **41** (2008) 135203 (23pp) doi:10.1088/1751-8113/41/13/135203

Boundary-condition-varying circle billiards and gratings: the Dirichlet singularity

M V Berry and M R Dennis

H H Wills Physics Laboratory, Tyndall Avenue, Bristol BS8 1TL, UK

Received 21 December 2007
Published 14 March 2008
Online at stacks.iop.org/JPhysA/41/135203

Abstract

Waves in a two-dimensional domain with Robin (mixed) boundary conditions that vary smoothly along the boundary exhibit unexpected phenomena. If the variation includes a 'D point' where the boundary condition is Dirichlet (vanishing wavefunction), a variety of arguments indicate that the system is singular. For a circle billiard, the boundary condition fails to determine a discrete set of levels, so the spectrum is continuous. For a diffraction grating defined by periodically varying boundary conditions on the edge of a half-plane, the phase of a diffracted beam amplitude remains undetermined. In both cases, the wavefunction on the boundary has a singularity at a D point, described by the polylogarithm function.

PACS numbers: 02.30.Tb, 02.30.Jr, 03.65.Ge

1. Introduction

The most general local Hermitian restrictions on wavefunctions in the presence of a hard wall are Robin, that is mixed, boundary conditions (Gustavson and Abe 1998), in which a real linear combination of the wavefunction and its normal derivative vanishes. The more familiar Dirichlet (vanishing wavefunction) and Neumann (vanishing normal derivative) conditions are special cases. In previous implementations (Sieber *et al* 1995, Berry and Ishio 2002), the boundary conditions have been either the same at all points on the boundary, or piecewise constant (for example, Dirichlet on an external billiard boundary and Neumann on an internal symmetry line, as in Berry (1981a)).

Here we will study two systems where the Robin conditions vary smoothly along the boundary of a two-dimensional domain within which a particle moves freely. Thus monochromatic waves with energy E satisfy

$$\nabla^2\psi + k^2\psi = 0, \qquad k^2 = E. \tag{1.1}$$

In the first system, the domain is the interior of the unit circle with coordinates $\{r, \phi\}$, and the boundary condition is

$$\kappa(\phi)\psi(1,\phi) + \frac{\partial}{\partial r}\psi(1,\phi) = 0, \tag{1.2}$$

where the function $\kappa(\phi)$ is real and 2π periodic. Therefore this system is a circle billiard, and we are interested in its bound states. In the second system, the domain is the upper half-plane $y \geqslant 0$, and the boundary condition on the x-axis for waves $\psi(x, y)$ is

$$\kappa(x)\psi(x,0) - \frac{\partial}{\partial y}\psi(x,0) = 0, \tag{1.3}$$

with the sign reflecting the same choice of normal (outwards) as in (1.2). If again the function $\kappa(x)$ is chosen to be real and 2π periodic, the x axis corresponds to a diffraction grating for plane waves incident from $y > 0$, and we study Bragg-diffracted beams. It is easy to show that requiring κ to be real is equivalent to the Hermiticity requirement that there is no current across the boundary.

We will often take κ proportional to the wavenumber k. As well as simplifying many of the formulae, this compensates semiclassically for the increase of the normal derivatives in (1.2) and (1.3); otherwise, almost all the high-lying (large k) states would effectively satisfy Neumann conditions. More precisely, when κ is proportional to k, (1.1) and (1.2) correspond not to a single Hamiltonian but to a family, in which κ depends on a parameter A. In the following, what we refer to as 'the spectrum' corresponds to the intersections of the line $A = k$ with the curves representing eigenvalues $\lambda(A)$ in the plane parameterized by $\sqrt{\lambda}$ and A.

Zeros of κ correspond to Neumann (N) points, and poles to Dirichlet (D) points. The simplest case exhibiting both, to be explored in detail later, is

$$\kappa(\phi) = k\cot\left(\tfrac{1}{2}\phi\right). \tag{1.4}$$

(Notwithstanding the half-angle, this is single valued-round the circle boundary, and with $\phi \to x$ the analogous grating is still 2π periodic.) There is a single D point, at $\phi = 0$, and a single N point, at $\phi = \pi$.

For any choice of $\kappa(\phi)$, the circle eigenstates are combinations of Bessel functions whose order n represents angular momentum; these are conveniently written as

$$\psi(r,\phi) = \sum_{n=-\infty}^{\infty} a_n \exp(\mathrm{i}n\phi)\frac{J_n(kr)}{J_n(k)}, \tag{1.5}$$

with the possible values of k determined by the application of (1.2).

In the grating case, it suffices for present purposes to consider only normal incidence, for which the total wave is

$$\psi(x,y) = \exp(-\mathrm{i}ky) + \sum_{n=-\infty}^{\infty} a_n \exp\{\mathrm{i}(nx + kr_n y)\}, \tag{1.6}$$

where now n denotes transverse linear momentum and the amplitudes a_n of the diffracted beams are determined by the application of (1.3), and

$$r_n \equiv \sqrt{1 - n^2/k^2}, \tag{1.7}$$

in which the square root is positive real for the propagating waves $|n| < k$, and positive imaginary for the evanescent waves $|n| > k$.

It might seem that varying κ merely adds complication to the cases of constant κ, with the innocuous effects of simply modifying the discrete spectra for the circle and the Bragg amplitudes for the grating. And this is indeed what happens if there are no D points. But

the presence of D points has a radical effect: it introduces a singularity into the Hamiltonian, which no longer generates discrete eigenvalues in the circle and fails to determine the Bragg amplitudes for the grating. This was unexpected and at first appeared paradoxical. Our aim here is to demystify what we will call the D singularity.

Section 2 revisits the familiar case of constant κ, emphasizing the peculiar nature of the limit $\kappa \to -\infty$, that is, approaching Dirichlet from the negative side. In section 3 we give some heuristic semiclassical reasons for regarding D points on the boundary as singularities, likely to have a dramatic effect.

Section 4 is a detailed study of the case (1.4) for the circle, which is expected to contain all essential features of more general billiards with D points. The spectrum of positive-energy states appears to be continuous; and the strategy of regarding the billiard with a D point as the limit of billiards with no D points, for which the spectrum is discrete, also fails to determine a discrete spectrum. The wavefunctions in the bound continuum states are well behaved everywhere except at the D point on the boundary, at which they have singularities described by the polylogarithm function, whose relevant asymptotics is developed in appendix A. Section 5 concerns boundaries without D points, where as expected the spectrum is discrete, but with some interesting features. The case where two D points coalesce is delicate: as we show in appendix B, the spectrum can be continuous or discrete, depending on a sign associated with the singularity.

Section 6 considers the diffraction grating with varying boundary conditions; if there is a D point, as in (1.4), the amplitudes of the diffracted beams in the wave (1.6) can all be calculated completely (after imposing Hermiticity on the Hamiltonian) except for the phase of one of them, which remains undetermined, even if the grating is regarded as the limit of one without D points.

The continuum reported here for the circle billiard is unfamiliar but not unprecedented. Smilansky (2004) showed similar behaviour in a quantum system with two freedoms, in which a particle moves in a harmonic oscillator potential coupled to a delta function; his conclusions were supported by rigorous analysis by Solomyak (2004). That example, whose main purpose was to illustrate a class of models exhibiting irreversibility, does not involve the D point singularity, with associated polylogarithm behaviour, that we are emphasizing here.

In order to keep this already long paper as concise as possible, we have omitted many technical details of the arguments. Moreover, we regard this paper as work in progress, that is exploratory: raising more issues than we have been able to settle here.

2. Constant Robin parameter

Here the importance of the D singularity becomes evident for the circle as $\kappa \to -\infty$, that is as the Dirichlet condition is approached from below. For constant κ, the circle billiard modes are

$$\psi_{nm}(r, \phi) = \exp(\mathrm{i}n\phi) J_n(k_{nm} r), \tag{2.1}$$

where the eigenvalues k_{nm} are the solutions of

$$F_n(E_{nm}) \equiv \sqrt{E} \frac{J_n'(\sqrt{E_{nm}})}{J_n(\sqrt{E_{nm}})} = -\kappa. \tag{2.2}$$

Figure 1 shows the functions $F_n(E)$, and some of the eigenvalues, given as intersections with the line $-\kappa$. The states with $n \neq 0$ are doubly degenerate because $F_n(E) = F_{-n}(E)$. For $\kappa > 0$ all states have positive E.

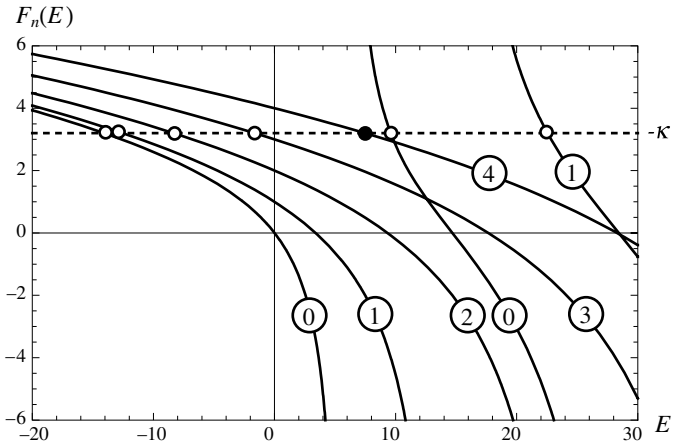

Figure 1. Positive and negative levels (white circles) and surface mode (black circle) for negative Robin parameter κ (dashed) for the Bessel functions J_n, $0 \leqslant n \leqslant 4$, calculated from (2.2).

When $\kappa < 0$, then, as is known (Balian and Bloch 1970), there are states with negative E. To find the number of such states, we note that

$$F_n(-E) = \sqrt{E}\frac{I_n'(\sqrt{E})}{I_n(\sqrt{E})} \tag{2.3}$$

takes the zero-energy values

$$F_n(0) = n. \tag{2.4}$$

Thus the number of negative-energy states is $2\mathrm{int}(-\kappa)$, and so grows without limit as $\kappa \to -\infty$.

This behaviour is consistent with the Weyl rule (Baltes and Hilf 1976), in which the Robin parameter affects the boundary term according to (Sieber *et al* 1995)

$$\mathcal{N}(k) = \frac{1}{4}k^2 + \frac{1}{2}k\left[2\left(\sqrt{1+\left(\frac{\kappa}{k}\right)^2} - \frac{\kappa}{k}\right) - 1\right] + \text{curvature term} + \cdots. \tag{2.5}$$

(Note that as $k \to \infty$ this reduces to the Neumann counting function, unless κ is proportional to k as mentioned previously.) The number $\mathcal{N}(0)$ of negative-energy states is given by

$$\mathcal{N}(k) \to 2|\kappa|\Theta(-\kappa) \qquad \text{as } k \to 0, \tag{2.6}$$

which diverges as the Dirichlet limit is approached from below, exactly as described above.

We note that the lowest positive-energy states for large negative κ (e.g., the black circle in figure 1) are concentrated near the boundary, because

$$J_n(kr) \approx J_n(k)r^n \approx J_n(k)\exp\{-|n|(1-r)\} \qquad (|n| \gg 1,\ 1-r \ll 1). \tag{2.7}$$

These states are the analogues of whispering-gallery modes for positive κ.

3. Semiclassical analysis for varying Robin parameter

For the circle billiard, κ has a simple pole at the simplest D point ϕ_{D}, and we can take

$$\kappa(\phi) \approx \frac{kD}{\phi - \phi_{\mathrm{D}}}. \tag{3.1}$$

In this case, the Weyl rule (2.5), generalized to incorporate variations of the boundary conditions, namely

$$\mathcal{N}(k) = \frac{1}{4}k^2 + \frac{1}{4\pi}k\int_0^{2\pi} \mathrm{d}\phi \left[2\left(\sqrt{1+\left(\frac{\kappa(\phi)}{k}\right)^2} - \frac{\kappa(\phi)}{k} \right) - 1 \right] + \cdots, \tag{3.2}$$

predicts infinitely many positive-energy states between any two wavenumbers k_1 and k_2:

$$\mathcal{N}(k_2) - \mathcal{N}(k_1) \approx \frac{1}{4}\left(k_2^2 - k_1^2\right) + \frac{1}{2}(k_1 - k_2) + (k_1 - k_2)\frac{D}{\pi}\int_0^{\phi_\mathrm{D}} \frac{\mathrm{d}\phi}{(\phi - \phi_\mathrm{D})} = \infty. \tag{3.3}$$

This is the first suggestion that the spectrum is continuous when there is a D point.

A physical picture of the origin of the D singularity for the circle follows from the observation, easy to check, that the general boundary-varying Robin condition is equivalent to a Neumann boundary, to which is added, just inside the boundary, a δ-function potential whose strength varies round the boundary. Explicitly, the potential for the circular billiard is

$$V(r, \phi) = \kappa(\phi)\delta(r - 1 + \varepsilon) \tag{3.4}$$

(this idea is reminiscent of the single-layer potential introduced by Balian and Bloch (1970)). Regarding the δ-function potential as the limit of a Gaussian, it is clear that a D point corresponds to a singularity where a potential barrier is infinitely high on the $\kappa > 0$ side, and a potential well is infinitely deep on the $\kappa < 0$ side; application of the Weyl rule to the potential well again predicts infinitely many states between any two positive energies, implying a continuous spectrum.

The following argument suggests that wavefunctions on the boundary will be singular at D points, and applies both to the circle and the grating. Consider waves with large momenta $|n| \gg k$. These are evanescent, that is, concentrated near the boundary (cf (2.7)), and, to satisfy the wave equation, are approximately local plane waves. In Cartesian coordinates,

$$\begin{aligned} \psi(x, y) &= \exp(\mathrm{i}nx)\exp\{-y\sqrt{n^2 - k^2}\} \\ &\approx \exp(\mathrm{i}nx)\exp\{-y|n|\}. \end{aligned} \tag{3.5}$$

Direct application of the boundary condition (1.3) gives

$$|n| + \kappa = 0, \tag{3.6}$$

so as expected these states can exist only when $\kappa < 0$. When κ varies, the natural WKB generalization of (3.5) leads, with (3.1) with $\phi \to x$, to a singularity:

$$\begin{aligned} \psi_\pm(x, 0) &\approx \exp\left\{ \pm\mathrm{i}\int^x \mathrm{d}x'|n(x')| \right\} \\ &= \exp\{\mp\mathrm{i}kD\log|x - x_\mathrm{D}|\}\Theta(D(x_\mathrm{D} - x)), \end{aligned} \tag{3.7}$$

where $\pm$ denotes the sign of n. Later we will show that the exact wavefunctions have precisely this singularity: oscillating infinitely fast as the D point is approached through negative κ values, discontinuously changing to a smooth function where κ is positive.

For the last of our preliminary indications that D points are special, consider reflection from the boundary, for non-evanescent waves, that is $|n| < k$, in the semiclassical limit $k \gg 1$. In this case, we can regard the (locally straight) boundary as the x axis, with waves in direction θ_0 (measured from the normal) incident from positive y.

When κ is constant, the total wave (incident+reflected) is

$$\psi(x, y) = \exp\{\mathrm{i}k(x\sin\theta_0 - y\cos\theta_0)\} + R(\kappa, \theta_0)\exp\{\mathrm{i}k(x\sin\theta_0 + y\cos\theta_0)\}, \tag{3.8}$$

with the reflection coefficient easily derived by the application of (1.4) to be

$$R(\kappa,\theta_0) = -\frac{(\kappa + \mathrm{i}k\cos\theta_0)}{(\kappa - \mathrm{i}k\cos\theta_0)} \equiv \exp\{\mathrm{i}\gamma(\kappa,\theta_0)\}. \tag{3.9}$$

When κ varies, we can still expect that short-wave reflections will be locally given by the same formula (a more careful analysis confirms this), so the wave in the boundary will be

$$\psi_{\mathrm{refl}}(x,0) \approx \exp\left\{\mathrm{i}\int^x \mathrm{d}x' k_x(x')\right\}, \tag{3.10}$$

in which the local transverse wavenumber is

$$k_x(x) = k\cos\theta_0 + \frac{\partial\gamma(\kappa(x),\theta_0)}{\partial x}. \tag{3.11}$$

The second term represents the momentum transferred to the reflected wave by the variation of the boundary condition, since this variation breaks the translational symmetry and momentum along the surface will no longer be conserved. The reflection will no longer be specular, and the momentum kick will be

$$\Delta k_x = \frac{\partial\gamma}{\partial x} = -\frac{2\kappa'(x)k\cos\theta_0}{\kappa(x)^2 + k^2\cos^2\theta_0}. \tag{3.12}$$

(Note that this is independent of k if κ is proportional to k.) This kick couples different angular momenta in the circle billiard, and generates Bragg-diffracted beams in the grating.

The sign of the kick depends on the sign of the derivative $\kappa'(x)$. On the average, representing the average angular-momentum kick in the circle case, the kick is

$$\begin{aligned}\langle\Delta k_x\rangle &= \frac{1}{2\pi}\int_0^{2\pi}\mathrm{d}x\frac{\partial\gamma}{\partial x} = -\frac{k\cos\theta_0}{\pi}\int_{\mathrm{C}}\frac{\mathrm{d}\kappa}{\kappa^2 + k^2\cos^2\theta_0} = -\frac{1}{\pi}\int_{\mathrm{C}}\frac{\mathrm{d}Q}{Q^2+1}\\ &= \text{winding number of } R(\kappa(x),\theta_0) \text{ as } x \text{ increases by } 2\pi.\end{aligned} \tag{3.13}$$

In this formula, C is the path traversed by κ (x) as x increases by 2π. If there are no D points, C is a series of self-retracing segments, and the average kick is zero. But if there are D points then C can consist of segments $-\infty < Q < +\infty$, each contributing unity to (3.13). Therefore D points are necessary in order for there to be a net momentum kick. In the circle case, this will result in reflected waves getting ever closer to glancing incidence, eventually (as k_x increases through k) becoming evanescent, that is concentrated near the boundary. In the grating, it will generate powerful evanescent waves. Note that the average kick (3.13) is independent of both θ_0 and k; it depends only on the topology of $\kappa(x)$.

In section 5 we will explore the implications of nonspecularity in more detail.

4. Spectrum with a Dirichlet singularity

An easy calculation shows that with the boundary condition (1.4) the coefficients in the superposition (1.5) satisfy the two-term recurrence relation

$$a_{n+1} = -a_n\frac{(1-\mathrm{i}\rho_n)}{(1+\mathrm{i}\rho_{n+1})}, \tag{4.1}$$

where

$$\rho_n(k) \equiv \frac{J_n'(k)}{J_n(k)}. \tag{4.2}$$

All a_n can be determined starting from any one of them, and it is convenient to choose $a_0 = 1$. Then

$$a_n = (-1)^n\frac{(1-\mathrm{i}\rho_0)}{(1+\mathrm{i}\rho_n)}\prod_{m=1}^{n-1}\frac{(1-\mathrm{i}\rho_m)}{(1+\mathrm{i}\rho_m)}. \tag{4.3}$$

With these a_n, we will soon see that the series (1.5) converges for any k, so the spectrum is continuous (even though the infinite bidiagonal determinant associated with (4.1) never vanishes).

It follows from (4.1) that

$$a_{-n} = a_n^*, \tag{4.4}$$

so the wavefunctions can be chosen to be real (as expected since the general boundary conditions (1.3) define a class of real operators, preserving the time-reversal symmetry), and given by

$$\psi(r,\phi) = \frac{J_0(kr)}{J_0(k)} + 2\,\mathrm{Re}\sum_{n=1}^{\infty} a_n \exp(\mathrm{i}n\phi)\frac{J_n(kr)}{J_n(k)}. \tag{4.5}$$

To understand these wavefunctions, we must consider the convergence of the series. For $n < k$, that is nonevanescent angular-momentum contributions, the a_n in (4.3) oscillate as n varies. In the evanescent regime, use of

$$\rho_n(k) \approx \frac{|n|}{k} \qquad (|n| \gg k) \tag{4.6}$$

leads to the following asymptotics of (4.3) in terms of an exactly calculated a_{n_0}:

$$a_n \approx a_{n_0}\frac{n_0}{n}\prod_{s=n_0+1}^{n-1}\frac{s+\mathrm{i}k}{s-\mathrm{i}k} \approx a_{n_0}\left(\frac{n_0}{n}\right)^{1-2\mathrm{i}k} \quad (n \gg k, n_0 \gg k). \tag{4.7}$$

Incorporating this into the tail of the series (4.5) gives the wavefunction as

$$\psi(r,\phi) = \frac{J_0(kr)}{J_0(k)} + 2\,\mathrm{Re}\sum_{n=1}^{n_0} a_n \exp(\mathrm{i}n\phi)\frac{J_n(kr)}{J_n(k)} + 2\,\mathrm{Re}\, a_{n_0} n_0^{1-2\mathrm{i}k}\sum_{n=n_0+1}^{\infty}\frac{r^n}{n^{1-2\mathrm{i}k}}\exp(\mathrm{i}n\phi). \tag{4.8}$$

The tail of the series can be expressed in terms of the polylogarithm function $\mathrm{Li}_\alpha(\beta)$ of complex order α and argument β:

$$\sum_{n_0+1}^{\infty}\frac{r^n}{n^{1-2\mathrm{i}k}}\exp(\mathrm{i}n\phi) = \mathrm{Li}_{1-2\mathrm{i}k}(r\exp(\mathrm{i}\phi)) - \sum_{n=1}^{n_0}\frac{r^n}{n^{1-2\mathrm{i}k}}\exp(\mathrm{i}n\phi). \tag{4.9}$$

Inside the circle, that is when $r < 1$, the series converges, and ψ is a smooth function of position. On the boundary $r = 1$, asymptotics of Li, given in appendix A, shows that ψ is smooth everywhere except at the D point $\phi = 0$, where it has precisely the singularity of the type (3.7) anticipated semiclassically. This singularity can also be obtained directly by replacing the tail of the series in (4.8) by an integral and approximating this using end-point asymptotics.

We note the intriguing fact that at its singularity, corresponding to the D point on the circle, the polylogarithm is given by the Riemann zeta function on the edge of the critical strip:

$$\mathrm{Li}_{1-2\mathrm{i}k}(1) = \zeta(1-2\mathrm{i}k). \tag{4.10}$$

This suggests that the requirement that the Dirichlet singularity is suppressed generates the Riemann zeros as resonances.

Figure 2 shows three wavefunctions, smooth almost everywhere but exhibiting oscillations near the boundary that get faster as the D point is approached from the negative side. Figure 3(*a*) shows the wavefunction on the boundary, with the series (4.5) simply truncated after 50 terms; figure 3(*b*) shows the effect of the polylogarithm regularization (4.8).

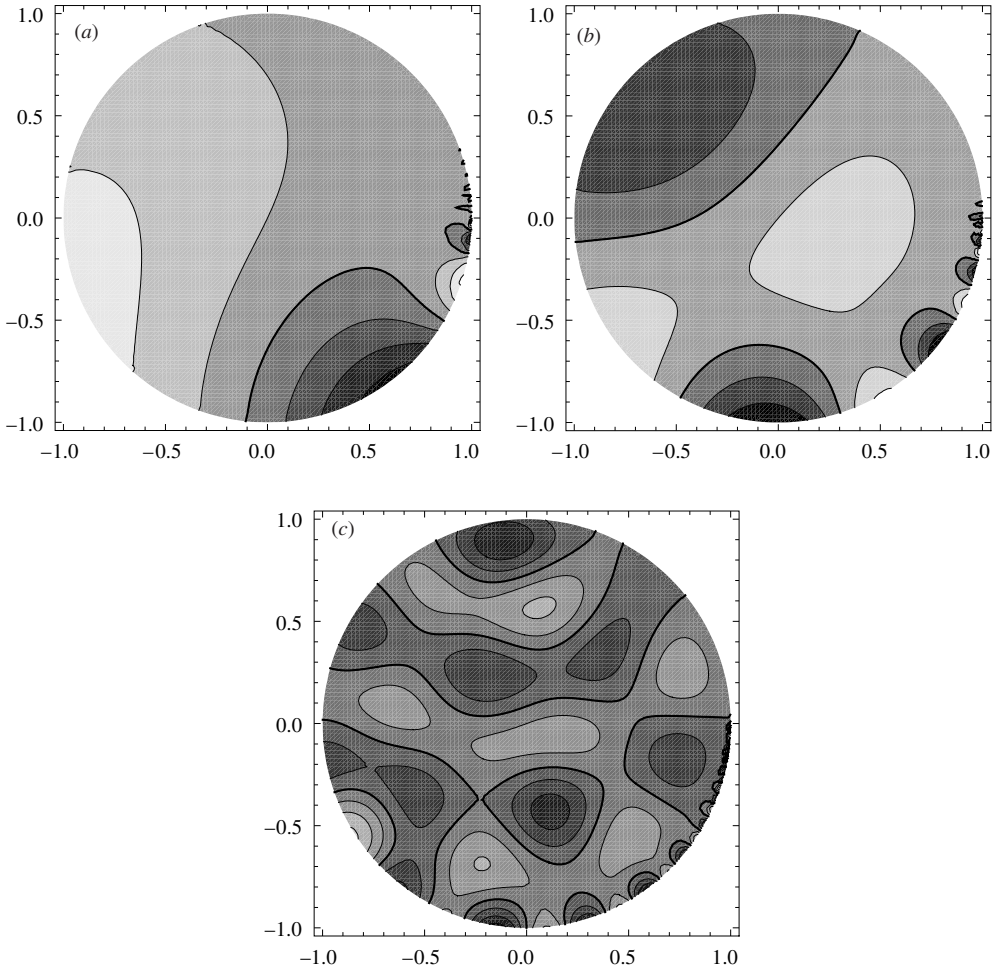

Figure 2. Contour plots of wavefunctions with boundary condition $\kappa(\phi) = k\cot(\phi/2)$, for (*a*) $k = 1.4$; (*b*) $k = 3.4$; (*c*) $k = 10$. The nodal lines are the thick curves.

These wavefunctions have been constructed to satisfy the boundary condition (1.4), and it is important to explore how accurately they do so. To examine this, we computed $k\psi/\partial_r\psi$ and compared this with the theoretical value $-\tan(\phi/2)$. As figure 4(*a*) illustrates, the accuracy is poor, even after including 500 terms of the regularized series for the same k as in figure 3. The reason is that on the boundary the normal derivative $\partial_r\psi$ is more singular than ψ itself, implying that although ψ converges the normal and tangential components of the local momentum do not. Just inside the boundary, however, the boundary condition is well satisfied, as figure 4(*b*) shows. This double regularization—polylogarithm tail of the angular-momentum series, and approaching the boundary from $r < 1$—deserves further study.

In a further attempt at regularization, we can regard the boundary condition (1.3) as the limit $\varepsilon \to 1$ of

$$\kappa(\phi) = k\frac{\sin\phi}{1-\varepsilon\cos\phi}. \tag{4.11}$$

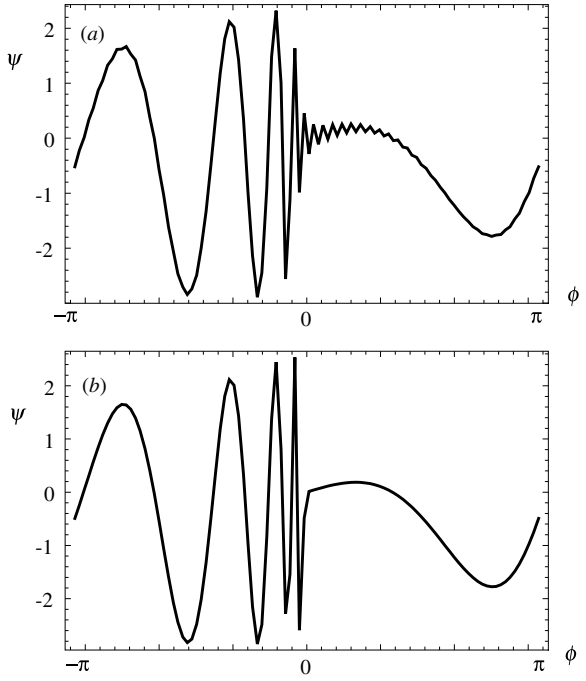

Figure 3. Boundary wavefunction $\psi(1,\phi)$ with boundary condition $\kappa(\phi) = k\cot(\phi/2)$, for $k = 3.4$: (*a*) including 50 terms of unregularized series (4.3); (*b*) as (*a*), including the polylogarithm regularization (4.8).

As figure 5 illustrates, there are no D singularities for $\varepsilon < 1$; the D singularity in (1.4) at $\phi = 0$ develops from an N point as $\varepsilon \to 1$ from below. For any fixed $\varepsilon < 1$, the coefficients a_n in (1.5) satisfy a three-term recurrence relation, corresponding to an infinite tridiagonal matrix whose determinant vanishes at a discrete set of real k which are the billiard eigenvalues. Numerically, truncation to an $N \times N$ matrix gives a determinant whose zeros converge as N increases. But the convergence gets worse as $\varepsilon \to 1$, and when $\varepsilon = 1$ there is no convergence, that is, the zeros depend on the truncation. Therefore the regularization (4.11) fails.

Nevertheless, it is interesting to examine briefly the three-term recurrence relation for $\varepsilon = 1$, namely

$$a_{n-1}(1 - \mathrm{i}\rho_{n-1}) + 2\mathrm{i}a_n\rho_n - a_{n+1}(1 + \mathrm{i}\rho_{n+1}) = 0, \tag{4.12}$$

with ρ_n defined by (4.2). As is easily confirmed, this is satisfied by any set of coefficients satisfying the two-term relation (4.1). But (4.12) has additional solutions. To study them, we note that if we write (4.1) in the form

$$F_n \equiv a_n(1 + \mathrm{i}\rho_n) + a_{n-1}(1 - \mathrm{i}\rho_{n-1}) = 0, \tag{4.13}$$

then (4.12) can be written as

$$F_{n+1} = F_n. \tag{4.14}$$

Thus F_n is a intriguing conserved quantity, whose value for the solution of (4.1) is zero but which in general can take any value F. However, asymptotic analysis, not given here, shows that when $F \neq 0$ the coefficients a_n tend to a constant for $|n| \gg k$, so the convergence

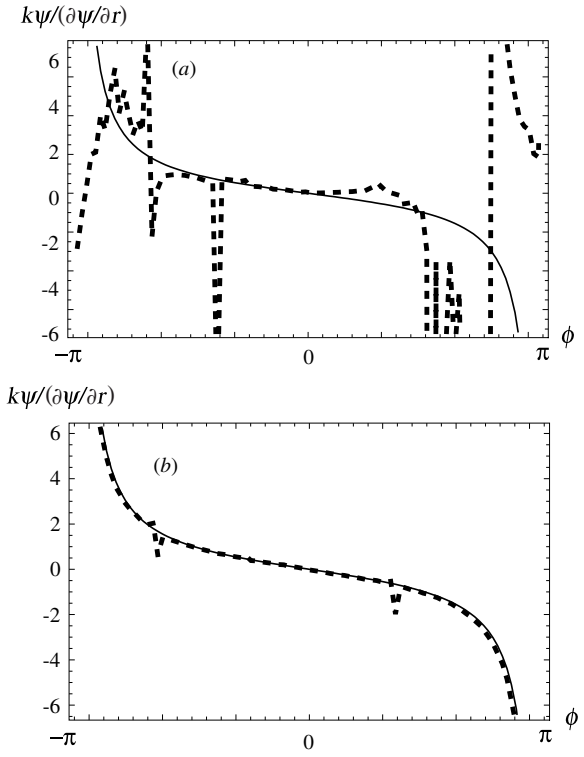

Figure 4. Dashed curves: computation of $k\psi/\partial_r\psi$ for the state with $k = 3.4$ with boundary condition $\kappa(\phi) = k\cot(\phi/2)$, including 500 terms of the regularized series (4.8); full curves: theoretical value $-\tan(\phi/2)$ (*a*) on the boundary $r = 1$; (*b*) close to the boundary $r = 0.98$.

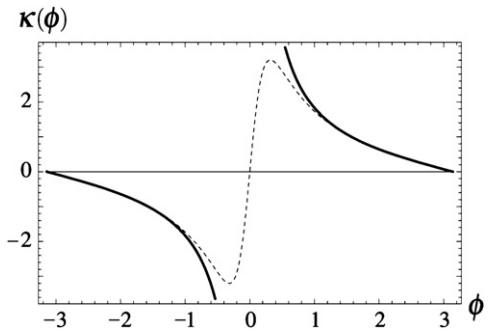

Figure 5. Full curve: boundary condition function (1.4) with a Dirichlet singularity at $\phi = 0$. Dashed curve: condition (4.11) for $\varepsilon = 0.95$, which has no Dirichlet singularity.

of the series (4.5) for the wavefunction on the boundary is worse than that leading to the polylogarithm (4.8).

The spectrum is continuous; nevertheless, the states ψ are square-integrable. This follows from (1.5), from which

$$\int_0^1 \mathrm{d}r\, r \int_0^{2\pi} \mathrm{d}\phi |\psi(r,\phi)|^2 = 2\pi \sum_{-\infty}^{\infty} |a_n|^2 \int_0^1 \mathrm{d}r\, r \frac{J_n^2(kr)}{J_n^2(k)}, \tag{4.15}$$

where

$$\int_0^1 \mathrm{d}r\, r \frac{J_n^2(kr)}{J_n^2(k)} \to \frac{1}{2|n|} \qquad (|n| \gg k) \tag{4.16}$$

and the asymptotic form (4.7), which implies

$$|a_n| \to \frac{\text{constant}}{n} \qquad (|n| \gg k). \tag{4.17}$$

5. Spectrum without a Dirichlet singularity

If there are no D points, the spectrum is discrete as in the more familiar case of constant κ, even in the presence of N points. As an example, in this section we explore the case

$$\kappa(\phi) = -k\cos\phi, \tag{5.1}$$

which has N points at $\phi = \pm\pi/2$ (up to a rotation, this is (4.11) with $\varepsilon = 0$). This operator possesses reflection symmetry about the x axis, and the states fall into parity-even (e) and parity-odd (o) classes, so that, in the representation (1.5)

$$\begin{aligned} \psi_{\mathrm{e}}(r,\phi) &= a_0 \frac{J_0(kr)}{J_0(k)} + 2\sum_{n=1}^{\infty} a_n \frac{J_n(kr)}{J_n(k)} \cos(n\phi) \\ \psi_{\mathrm{o}}(r,\phi) &= 2\sum_{n=1}^{\infty} a_n \frac{J_n(kr)}{J_n(k)} \sin(n\phi). \end{aligned} \tag{5.2}$$

In both classes, the coefficients satisfy the three-term recurrence relation

$$a_{n+1} + a_{n-1} - 2a_n\rho_n(k) = 0, \tag{5.3}$$

where ρ_n is defined in (4.2).

However, the initial conditions are different:

$$\left.\begin{array}{lll} a_0 = 1, & a_1 = \rho_0(k) & (\psi_{\mathrm{e}}) \\ a_0 = 0, & a_1 = 1 & (\psi_{\mathrm{o}}) \end{array}\right\}. \tag{5.4}$$

The wavenumbers k of eigenstates are determined by the vanishing of the tridiagonal determinant underlying (5.3), but it is convenient here to employ the equivalent condition that the coefficients must converge as $n \to \infty$. By (4.6), the asymptotic coefficients satisfy

$$a_{n+1} + a_{n-1} - \frac{2n}{k} a_n = 0 \qquad (n \gg k). \tag{5.5}$$

The solution (Abramowitz and Stegun 1972) is a superposition of J and Y Bessel functions:

$$a_n \approx A(k)J_n(k) + B(k)Y_n(k) \qquad (n \gg k). \tag{5.6}$$

Since $Y_n(k)$ grows factorially with n, eigenvalues are determined by the vanishing of the coefficient $B(k)$, which in turn is given in terms of any pair of asymptotic a_n by

$$B(k) = \frac{2}{\pi k} \lim_{n\to\infty} [a_n(k)J_{n+1}(k) - a_{n+1}(k)J_n(k)]. \tag{5.7}$$

As figure 6 illustrates, the zeros are easily identified. It is convenient to represent energy in the form

$$E \equiv \tfrac{1}{8}k^2, \tag{5.8}$$

so that the mth level in each class, according to the area term in the Weyl rule, is approximately $E_m \sim m$. Figure 7 shows two representations of a high-lying state. There is a strong

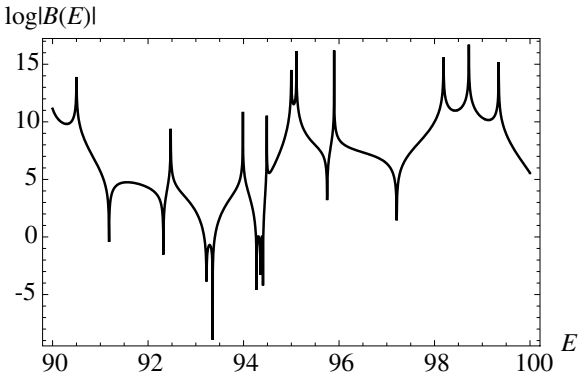

Figure 6. Coefficient B in (5.7) for even states with boundary condition $\kappa(\phi) = -k\cos\phi$, as a function of wavenumber $k = \sqrt{(8E)}$. The negative spikes correspond to eigenstates.

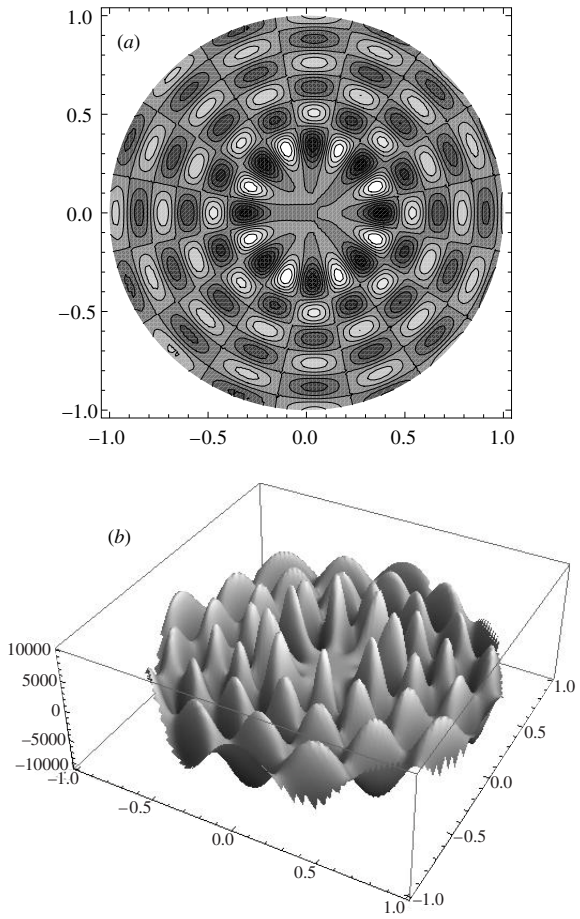

Figure 7. Even state $E_{110} = 97.206\,986\,712$ for boundary condition $\kappa(\phi) = -k\cos\phi$: (*a*) contour plot; (*b*) 3D plot.

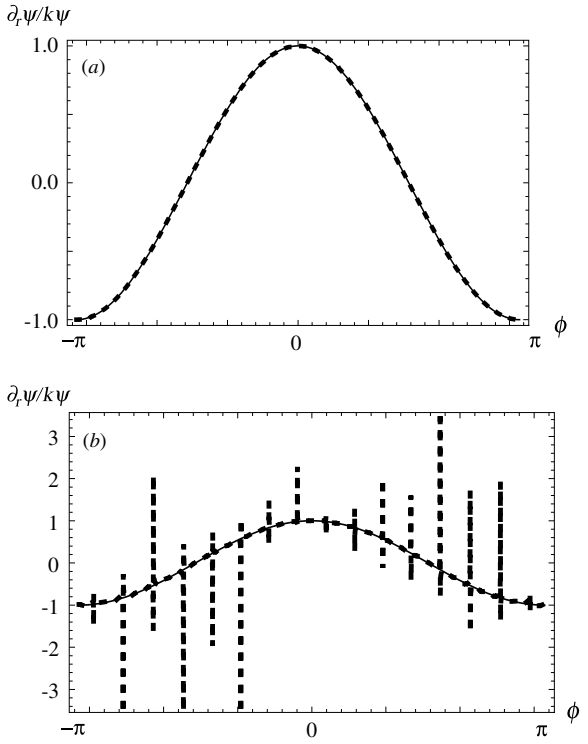

Figure 8. Dashed curves: computation of $\partial_r\psi/k\psi$ on the boundary for the 110th even state; full curves: theoretical value $\cos\phi$ (*a*) energy E_{110}; (*b*) $E_{110} + 10^{-8}$.

pattern, resembling a displaced Bessel mode and therefore suggesting near-integrability, but close examination shows that the nodal lines do not cross, so the states are not separable. Figure 8(*a*) shows that the boundary condition (5.1) is satisfied, but, as figure 8(*b*) shows, the agreement is destroyed by only a slight deviation (10^{-8} of the mean spacing).

The eigenstates are those of a semicircle billiard with the boundary condition (5.1) on the curved part of the boundary and Neumann (even states) or Dirichlet (odd states) on the diameter. Thus, from (2.5) applied to the present case, the first two terms of the Weyl series are

$$\mathcal{N}(E) = E + \frac{\sqrt{8E}}{2\pi}\left(\frac{1}{4}\int_0^{2\pi} \mathrm{d}\phi\,(2\sqrt{1+\cos^2\phi}-1) \pm 1\right)$$
$$= E + \frac{\sqrt{8E}}{2\pi}\left(2\sqrt{2}\mathrm{E}\left(\frac{1}{2}\right) - \frac{\pi}{2} \pm 1\right) = E + \sqrt{E}(1.012\,59 \pm 0.450\,16), \tag{5.9}$$

where E denotes the complete elliptic integral and +/− refer to the even/odd states.

The second term of the Weyl series implies that there are more even than odd states. The extra even states generalize the $n = 0$ Neumann states in (2.1), which have no odd counterparts. Unexpectedly, these 'rogue states' have an explicit analytic form. In terms of the zeros $j_{1,n}$ of the Bessel function J_1, the rogue energy E_n and wavefunction ψ_n of the nth such state are

$$E_n = \tfrac{1}{8}j_{1,n}^2,$$
$$\psi_n(r,\phi) = J_0(j_{1,n}r) + \frac{J_0(j_{1,n})}{J_1'(j_{1,n})}J_1(j_{1,n}r)\cos\phi, \tag{5.10}$$

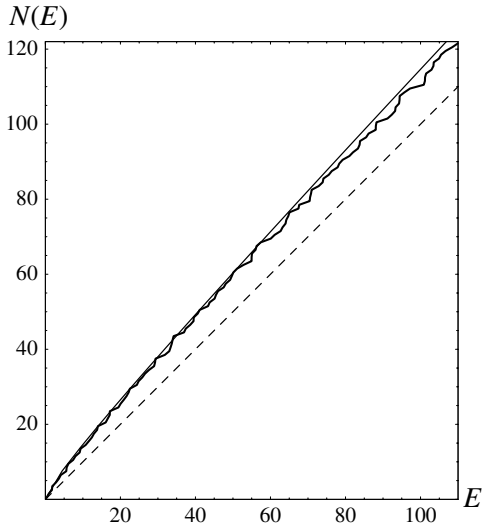

Figure 9. Thick curve: spectral staircase $\mathcal{N}(E)$ for even states with boundary condition $\kappa(\phi) = -\cos\phi$, as a function of E corresponding to wavenumber $k = \sqrt{(8E)}$; dashed curve: $N(E) = E$, corresponding to the area term in the Weyl series; full thin curve: $\mathcal{N}(E) = E + 0.571\,43\sqrt{E}$, corresponding to the area+perimeter term.

and it can be confirmed by direct calculation that these satisfy the boundary condition (5.1). (These rogue states are not captured by the numerical search technique based on (5.7), or the analogous tridiagonal determinant, for a technical reason associated with the appearance of $J_1(k)$ in the denominator in (5.2)).

In this way, we identified the lowest 122 even states. Comparison with (5.9) (figure 9) shows reasonable agreement, although the slight shortfall leaves open the possibility that some of the additional even states might have been missed (the next term of the Weyl series, arising from the curvature and corners of the semicircle, is too small to affect the comparison). Analogous calculations for the odd states are perfectly in agreement with (5.9).

As a preliminary indication of the spectral statistics, figure 10 shows the cumulative distribution

$$C(E) \equiv \int_0^S \mathrm{d}S' P(S') \tag{5.11}$$

of the nearest-neighbour level spacings S. The reasonable agreement with the Poisson distribution $P(S) = \exp(-S)$ suggests that the states are not chaotic, or at most weakly so. To identify the spectral statistics definitively (for example, to distinguish between Poisson and semi-Poisson), more data would be needed.

A heuristic explanation is based on the nonspecularity of reflection of local plane waves, discussed in section 3 (equation (3.11)). This implies that for particles incident at ϕ_0 on the boundary the incidence and reflection angles θ_0 and θ_1 are related by the law

$$\sin\theta_1 = \sin\theta_0 + \frac{1}{k}\frac{\partial\gamma}{\partial x} = \sin\theta_0 - \frac{2\kappa'(x)k\cos\theta_0}{k(\kappa(x)^2 + k^2\cos^2\theta_0)}. \tag{5.12}$$

Thus the nonspecularity is of order $1/k$. Although interpreting this in classical terms is problematic, it does seem reasonable to take it seriously, at least for the orbits of length less than k (corresponding to the Heisenberg time connected to the level spacing). Preliminary

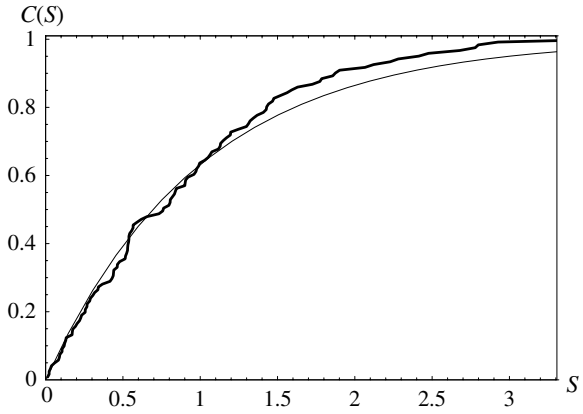

Figure 10. Thick curve: cumulative spacings distribution $C(S) \equiv \int_0^S \mathrm{d}S' P(S')$ of first 122 even levels of boundary condition $\kappa(\phi) = -\cos\phi$; thin curve: Poisson distribution $1 - \exp(-S)$.

exploration of the (non-symplectic) billiard boundary map determined by (5.12), whose phase space (Berry 1981b) has angular momentum $\sin\theta$ and coordinate ϕ, suggests that there is very little chaos. Our tentative conclusion is that the quantum system determined by (5.1) is only weakly nonintegrable.

A familiar phenomenon for two-dimensional systems is that energies of states belonging to different symmetry classes can coincide. In the system (5.1), this cannot happen (except for the rogue states (5.10)). This no-crossing phenomenon is familiar in one-dimensional systems, and can be understood in a similar way, starting from the three-term recurrence relation (5.3). We can think of (5.3) as a linear map in the plane $\{a_n, a_{n+1}\}$, with even and odd levels determined by different initial conditions (5.4) representing lines in the plane. The vanishing of the coefficient $B(k)$ (equation (5.7)) cannot occur simultaneously for the even and odd states. An implication is that in generalizations of (5.1) for which the boundary condition depends on a parameter and the coefficients are still determined by a three-term recurrence relation, there can be no level crossings; an example is (4.11) with $0 \leqslant \varepsilon < 1$.

To further clarify the significance of the absence of D points in (5.1), we briefly consider the analogous boundary condition with D points but no N points:

$$\kappa(\phi) = -\frac{1}{k\cos\phi}. \tag{5.13}$$

With the slightly modified representation

$$\psi(r,\phi) = \sum_{n=-\infty}^{\infty} b_n \exp(\mathrm{i}n\phi)\frac{J_n(kr)}{J_n'(k)}. \tag{5.14}$$

The recurrence relation analogous to (5.3) is

$$b_{n+1} + b_{n-1} = 2\frac{b_n}{\rho_n(k)} \approx 2b_n\frac{k}{n} \qquad (n \gg k). \tag{5.15}$$

Note that $\rho_n(k)$ has been replaced by $1/\rho_n(k)$. This is crucial, because the asymptotic solution replacing (5.6) is

$$b_n \sim A(+\mathrm{i})^n + B(-\mathrm{i})^n, \tag{5.16}$$

which cannot generate discrete eigenvalues. The difference between (5.6) and (5.16) is analogous to the distinction between classically forbidden and allowed regions in one dimension, which similarly underlies discrete and continuous spectra in one dimension.

As in previous sections, we included the eigenvalue k in (5.1) in order to simplify the formulae. We have also studied the case in which k is replaced by a constant parameter A, representing a family of Hermitian Hamiltonians. In the analogue of the Weyl formula (5.9), obtained from (3.2), the perimeter term does not vanish at $k = 0$; its value (for the even and odd states) is A/π, and represents the negative-energy states. Numerical computations confirm that if these are included in the count, the total number of even or odd states again agrees with predictions of the Weyl formula. The rogue states (5.10) now exhibit the unexpected feature that their energies are independent of the parameter A.

The relation between the case considered in this section, where there is no D singularity and the spectrum is discrete, and that of section 4, where the D singularity leads to a continuum, is clarified by considering the case where two D points coalesce, for example

$$\kappa(\phi) = \frac{\varepsilon k}{\sin^2\left(\frac{1}{2}\phi\right)}, \qquad \varepsilon = \pm 1. \tag{5.17}$$

This is studied in appendix B, where we show that the spectrum is continuous for $\varepsilon = -1$ and discrete for $\varepsilon = +1$, emphasizing what we have already discovered, that the singularity is associated with the approach to the D point from the negative side, that is $\kappa \to -\infty$.

6. Boundary-varying gratings

For most of this section, it will suffice to consider the grating wave (1.6) and (1.7) for normal incidence. With the boundary condition (1.4) with x replacing ϕ, the coefficients satisfy the inhomogeneous two-term recurrence relation

$$a_{n+1}(1 + r_{n+1}) + a_n(1 - r_n) + 2\delta_{n,0} = 0. \tag{6.1}$$

Consider first the forward-diffracted beams, that is $n > 0$. Noting $r_0 = 1$, forward recursion gives

$$a_1 = -\frac{2}{1 + r_1}, \qquad a_{n>0} = -\frac{2}{(1 + r_n)} \prod_{j=1}^{n-1} \frac{(r_j - 1)}{(r_j + 1)}. \tag{6.2}$$

The intensities of these forward beams decrease rapidly until the grazing-emergence beam $n = \text{int}\,[k]$. For the deep-evanescent waves $n \gg k$, use of

$$r_n \sim \mathrm{i}\frac{|n|}{k} \qquad (|n| \gg k) \tag{6.3}$$

(cf (4.6)), leads to (cf (4.7))

$$a_n \approx a_{n_0} \left(\frac{n_0}{n}\right)^{1-2\mathrm{i}k} (n \gg k, n^* \gg k), \tag{6.4}$$

and thence, through the positive-n terms in (6.2), to a polylogarithm singularity in the boundary wave $\psi(x, 0)$.

A difficulty arises with the terms $n \leqslant 0$, that is, the beams diffracted towards negative x. The recurrence relation (6.1) gives

$$a_{-1} = \frac{2a_0}{r_1 - 1}, \qquad a_{-n} = \frac{2a_0}{(r_n - 1)} \prod_{j=1}^{n-1} \frac{(r_j + 1)}{(r_j - 1)} \qquad (n > 1), \tag{6.5}$$

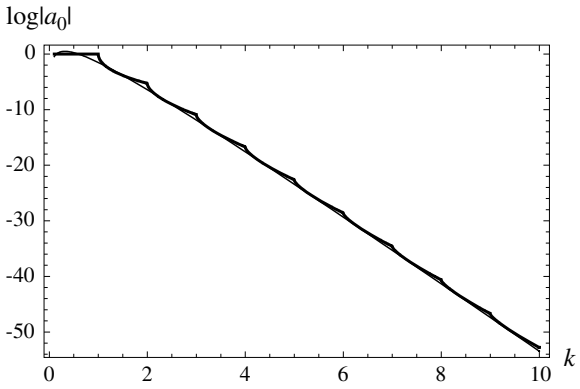

Figure 11. Thick curve: modulus $|a_0(k)|$ of a specular-reflected grating amplitude, calculated from (6.7); thin curve: the approximation (6.8).

leaving a_0 undetermined. The modulus $|a_0|$ can be determined by Hermiticity, in the form of the requirement that the incident and scattered y components of the current are equal. The condition, involving only the propagating waves with $|n| < k$, is

$$\sum_{|n|<k} |a_n|^2 r_n = 1. \tag{6.6}$$

It then follows from (6.5) after some calculation that

$$|a_0| = \prod_{n=1}^{\text{int}\,k} \left| \frac{r_n - 1}{r_n + 1} \right|^2. \tag{6.7}$$

For $k < 1$, $|a_0| = 1$, as is obvious since $n = 0$ is the only propagating diffracted beam. As k increases, $|a_0|$ decreases rapidly. This decrease can be approximated by using the Euler–Maclaurin formula to replace the sum in the $\log|a_0|$ by an integral. The result (replacing n/k by the integration variable t) is

$$|a_0| \approx \exp\left\{ 2k \int_{1/2k}^{1} \mathrm{d}t \, \log\left[\frac{1 - \sqrt{1-t^2}}{1 + \sqrt{1-t^2}} \right] \right\} \approx (4k\mathrm{e})^2 \exp(-2\pi k). \tag{6.8}$$

As figure 11 shows, this is an excellent approximation for all $k > 1$.

The asymmetry between Bragg beams with positive and negative n for this case of normal incidence, indicating a lop-sidedness of the diffraction, implies that the grating violates Friedel's law of crystallography, according to which the diffracted beam intensities would be invariant under the replacement of $\kappa(x)$ by $\kappa(-x)$. Such asymmetry also occurs in an exactly-solvable model of a non-Hermitian grating, and in echelette (blazed) gratings (Berry 1998, Born and Wolf 2005).

It follows from (6.7) and (6.8) that the a_n for $n \leqslant 0$ are very small for large k, that is in the semiclassical (geometrical optics) regime. These small values are not captured by a crude argument based on Kirchhoff diffraction, which predicts zero. In this approximation, the reflected wave is given simply by the incident wave at $y = 0$ (in this case $\psi_{\text{inc}} = 1$) multiplied by the local reflection coefficient (3.9). For the present case ($\theta_0 = 0$), this gives

$$\psi_{\text{refl,Kirchhoff}}(x, 0) = -\frac{\left(\cot\frac{1}{2}x + \mathrm{i}\right)}{\left(\cot\frac{1}{2}x - \mathrm{i}\right)} = -\exp(\mathrm{i}x), \tag{6.9}$$

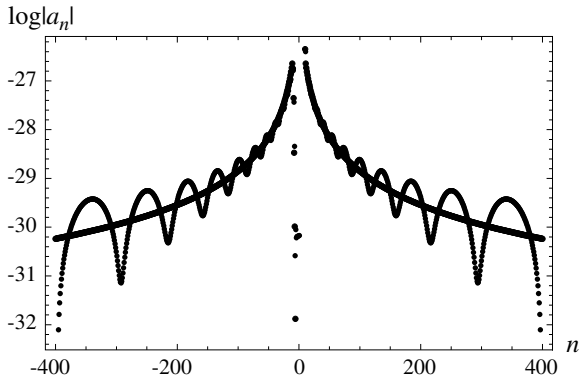

Figure 12. Oscillatory curve: coefficients a_n for $k = 10.2$, computed by inversion of the matrix in (6.10), truncated at $|n| = 400$; the oscillations are artefacts depending on the truncation. Smooth curve: coefficients computed analytically from (6.2) and (6.5) with $|a_0|$ calculated from (6.7).

corresponding, according to (1.6), to the single diffracted beam $n = 1$ with $a_1 = -1$, consistent with (6.2) and (6.5) for $k \gg 1$ assuming that a_0, and hence all the negative coefficients, are zero.

With (6.2), (6.5) and (6.7) the beam amplitudes are completely determined except for the phase $\arg a_0$. Careful examination of more sophisticated versions of Hermiticity, such as the grating analogue of the optical theorem (unitarity of the scattering matrix), even those involving evanescent waves (Brown *et al* 1982), also fail to determine this phase.

The regularization (4.11), with x replacing ϕ and $\varepsilon < 1$, fails too, in an interesting way, as does the analogous regularization described at the end of section 4. When $\varepsilon < 1$, (4.11) leads to a three-term recurrence relation whose associated tridiagonal matrix can be inverted, and the resulting a_n converge as the matrix size increases. But the convergence gets worse as $\varepsilon \to 1$, and fails when $\varepsilon = 1$. For this case, where the recurrence relation is

$$a_{n-1}(1 - r_{n-1}) + 2a_n r_n - a_{n+1}(1 + r_{n+1}) = 2\delta_{n,0} - 2\delta_{n,1}, \tag{6.10}$$

the convergence is illustrated in figure 12. This shows the evanescent amplitudes oscillating as they decay; the oscillations are self-similar, and increasing N produces graphs that look similar. In fact the oscillations are artefacts of the truncation: as N increases, the oscillations for fixed n get weaker. We have seen this numerically, and a long analytical argument, not given here and involving a conserved quantity analogous to (4.13) for the circle, shows that matrix inversion gives $\arg a_0$ proportional to $4k \log N$, and therefore truncation dependent.

This failure to determine $\arg a_0$ suggests that reflection from the grating is not well determined by the boundary condition (1.4). That the situation is exquisitely delicate is shown by the case of oblique illumination, where the incident beam has x dependence $\exp(\mathrm{i}n_0 x)$, and the diffracted beam amplitudes are denoted $a(n, n_0)$ (normal incidence is $n_0 = 0$). Lengthy but elementary analysis (again not given here) shows the following. For $n_0 < 0$, all amplitudes can be determined unambiguously; the only nonzero a_n are those with $n_0 \leqslant n \leqslant 0$. For $n_0 > 0$, the reflected waves for $n > 0$ can be determined explicitly, that is without phase or other ambiguity, and their amplitudes are nonzero only for $n \geqslant n_0$, meaning that for $n_0 \geqslant 2$ there are no diffracted beams with $n = 1, 2, \ldots, n_0 - 1$. The amplitudes with $n \leqslant 0$ cannot be determined explicitly, but they can all be expressed in terms of the zero coefficient

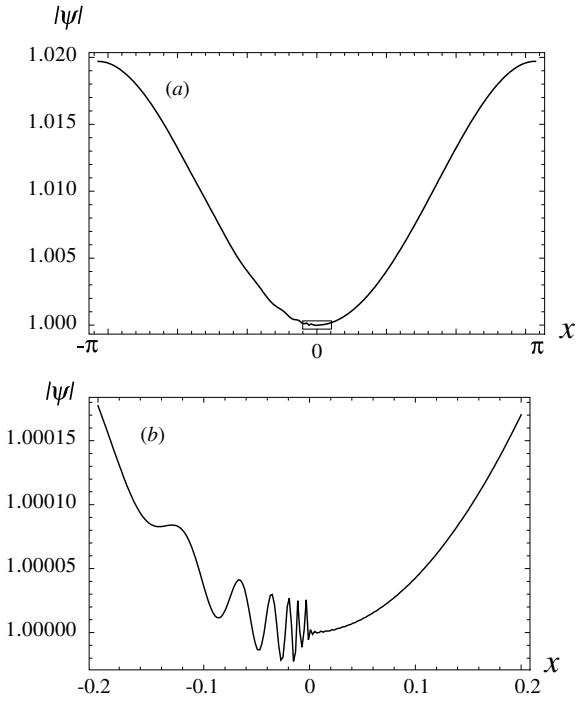

Figure 13. Wavefunction $|\psi(x, 0)|$ in the grating, calculated from the series (1.6) including terms $|n| < N$ with coefficients determined by the matrix inversion of (6.10), truncated at $N \times N$, for $k = 5.2$: (a) calculated with $N = 500$ shows the whole range $-\pi \leqslant x \leqslant \pi$; note that $|\psi|$ is close to unity, and the polylogarithm singularity is almost indiscernable; the magnification of the box near the origin (b), calculated with $N = 5000$, shows the polylogarithm singularity clearly.

a_{0,n_0}(representing normal reflection). This in turn can be simplified by using reciprocity, conveniently expressed in the form (Brown *et al* 1982)

$$r_n a_{n,n_0} = r_{n_0} a_{-n_0,-n}, \tag{6.11}$$

representing time reversal symmetry. Reciprocity enables all a_{0,n_0} to be expressed in terms of $a_{0,0}$, that is our previous a_0, whose phase remains undetermined.

Nevertheless, even for normal incidence the wavefunction (1.6) can still be calculated by inversion of the truncated matrix, and the slow convergence again generates a polylogarithm singularity at the D point $x = 1$. However, unless k is very small the wave on the boundary is almost constant (because a_1 is very close to unity and all other a_n are very small). Therefore very high magnification is required to display the singularity, as figure 13 illustrates. (The ambiguity in arg a_0 does not seem to affect the form of this singularity.)

7. Concluding remarks

Our main result has been the identification of an isolated D point, whose neighbourhood $\kappa \to -\infty$, as a singularity, and the elucidation of some of its consequences. This was unanticipated, because the superficially more singular situation, of the entire boundary consisting of D points, is the commonplace and unproblematic Dirichlet boundary condition.

Our exploration of varying boundary conditions suggests several areas for further investigation. Most urgent is a fuller understanding of the D singularity, in particular its role in generating a spectrum for the circle billiard and the physical reason why it implies a failure to determine arg a_0 for the grating. Here we admit that our arguments have been non-rigorous, and could benefit from the attention of mathematicians.

For billiards with no D points on the boundary, as in the case studied in section 5 and (4.11) with $\varepsilon < 1$, the spectrum is discrete and appears to be nonintegrable but only weakly so. It would be interesting to understand this fully, and in particular see if it can be explained by local nonspecular semiclassical reflection as conjectured in section 5. And calculation of more levels than the lowest 122 would enable more precise identification of the statistics.

For gratings without D points, there is no ambiguity in determining the beam amplitudes, and some choices of $\kappa(x)$ could lead to a class of exactly solvable models. It would be interesting to know if boundary-varying gratings could be implemented using metamaterials.

We have explored the simplest cases, but there are several obvious variants. Instead of the grating, we could consider the exterior problem of scattering of waves incident on the circle billiard from outside, especially in the context of inside–outside duality (Eckmann and Pillet 1995, Dietz *et al* 1995). And instead of the interior circle billiard, we could consider bound states in the truncated cylinder $\{0 \leqslant x \leqslant 2\pi\}$, $\{0 < y < 1\}$, with the varying boundary condition specified by a periodic $\kappa(x)$ at $y = 0$ and some other boundary condition at $y = 1$ (e.g. Dirichlet, or Neumann, or that specified by $\kappa(x)$, or the twisted case $\kappa(-x)$). These variants are interesting, but our examination of some of them indicates that the fundamental phenomena associated with the D singularity are the same as in the cases we describe here.

Acknowledgments

We thank John Hannay for discussions, Shmuel Fishman for discussions in the early stages of this work, Uzy Smilansky, in particular for drawing our attention to his paper (Smilansky 2004) and emphasizing the need to investigate regularizations such as (4.11), and Jon Keating for a suggestion that led to appendix B. Our research is supported by the Royal Society and Bristol University. In addition, MVB thanks the Solvay Institute, and MRD thanks the Lewiner Institute for Theoretical Physics and the Minerva Center at the Technion, for hospitality during this work.

Appendix A. Polylogarithm asymptotics

First, we seek to approximate the polylogarithm on the unit circle. Following the analogous procedure (Berry 1986, Berry and Keating 1990) for the Riemann zeta function, suggested by the special case (4.10), the first step is to truncate the defining sum at the Nth term, and represent the tail in terms of the Poisson summation formula:

$$\mathrm{Li}_{1-2\mathrm{i}k}(\exp(\mathrm{i}\phi)) = \sum_{n=1}^{N} \frac{1}{n^{1-2\mathrm{i}k}} \exp(\mathrm{i}n\,\phi) + \sum_{m=-\infty}^{\infty} \int_{N+\frac{1}{2}}^{\infty} \frac{\mathrm{d}s}{s} \exp\{\mathrm{i}(\phi - 2\pi m + k\log s)\}\,. \tag{A.1}$$

For large k, the integrals are oscillatory, so we can apply the method of stationary phase. The stationary points are

$$s_{\mathrm{c}} = \frac{2k}{2\pi m - \phi}. \tag{A.2}$$

The simplest procedure is to include only those terms m for which s_c lies in the range of integration. This restricts the sum according to

$$s_c > N \qquad \text{if} \quad \frac{1}{2}(1+\operatorname{sgn}\phi) \leqslant m < \frac{k}{\pi N} \qquad (0 < \phi \leqslant \pi). \tag{A.3}$$

The central feature, giving rise to the singularity at $\phi = 0$, is that the $m = 0$ term contributes if $\phi < 0$ but not if $\phi > 0$. The most economical representation, in which both series in (A.1) have the same number of terms, is obtained by choosing $N = \operatorname{int}\sqrt{(k/\pi)}$.

Application of the stationary phase gives the formula

$$\begin{aligned}\operatorname{Li}_{1-2ik}(\exp(i\phi)) \approx & \sum_{n=1}^{\operatorname{int}\sqrt{k/\pi}} \frac{1}{n^{1-2ik}} \exp(in\,\phi) \\ & + \Gamma(2ik)\exp\left(\frac{1}{2}k\right) \sum_{m=\frac{1}{2}(1+\operatorname{sgn}\phi)}^{\operatorname{int}\sqrt{k/\pi}} (2\pi m - \phi)^{-2ik}.\end{aligned} \tag{A.4}$$

Explicitly, the singularity given by the $m = 0$ term is

$$\exp\{-2ik\log|\phi|\}\,\Theta(-\phi), \tag{A.5}$$

which is precisely of the form (3.7) conjectured semiclassically.

Inside the unit circle, the procedure is similar, but with the crucial difference that the stationary point in the $m = 0$ integral moves smoothly past the end point as ϕ passes through zero. Therefore this integral must be approximated more carefully. The result is the more general approximation

$$\begin{aligned}\operatorname{Li}_{1-2ik}(w) \approx & \sum_{n=1}^{\operatorname{int}\sqrt{k/\pi}} \left(\frac{w^n}{n^{1-2ik}} + \Gamma(2ik)(-\log w + 2\pi i n)^{-2ik}\right) \\ & + \frac{1}{2}\Gamma(2ik)(-\log w)^{-2ik}\operatorname{Erfc}(S(w)),\end{aligned} \tag{A.6}$$

in which the argument is

$$S(w) = \exp\left(-\frac{1}{4}i\pi\right)\left[\frac{\log w}{2\sqrt{\pi}} + \sqrt{k}\exp(i\arg\log w)\right] \qquad (|\arg w| < \pi). \tag{A.7}$$

As figure 14 illustrates, these approximations capture the singularity that develops at $\phi = 0$ as r approaches 1.

Appendix B. Coalescing D points

For a circle billiard with coalescing D points, we use the model (5.17), in which $\varepsilon = +1$ represents a singularity with $\kappa \to +\infty$ and $\varepsilon = -1$ represents $\kappa - \infty$. It is convenient to represent the wave in the form (slightly different from (1.5))

$$\psi(r,\phi) = \sum_{n=-\infty}^{\infty} b_n \exp(in\,\phi)\frac{J_n(kr)}{J_n'(k)}. \tag{B.1}$$

Then the recurrence relation for the coefficients is

$$b_{n+1} + b_{n-1} = 2\left(\frac{2\varepsilon}{\rho_n} + 1\right)b_n \equiv 2A_n b_n, \tag{B.2}$$

in which ρ_n is defined by (4.2).

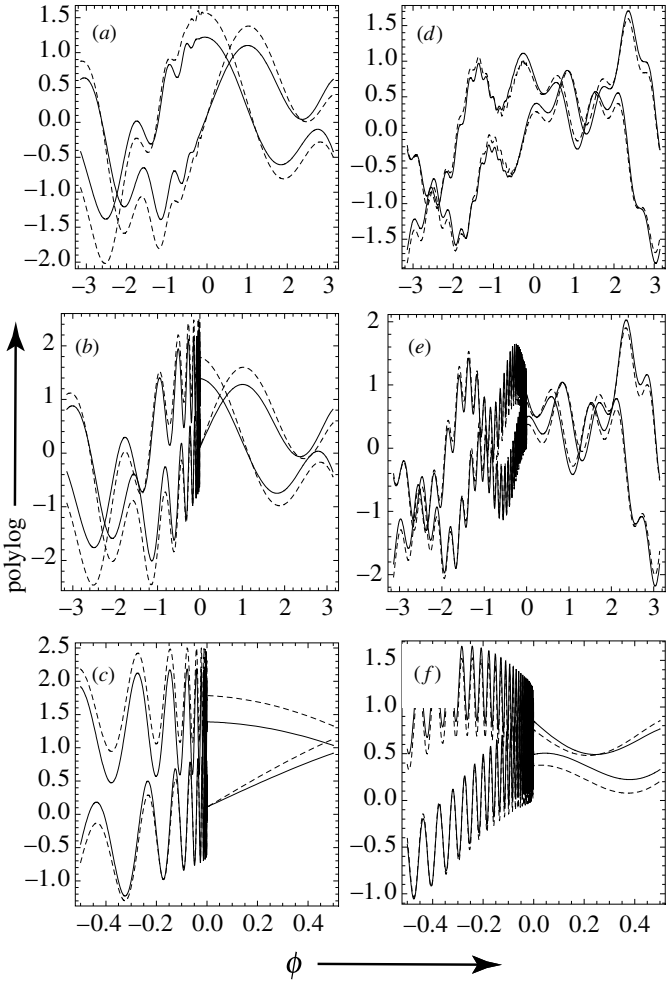

Figure 14. Polylogarithm $\mathrm{Li}_{1-2\mathrm{i}k}(r\exp(\mathrm{i}\phi))$ (full curves) and approximation (A.6) and (A.7) (dashed curves), with Re(Li) thick and Im(Li) thin. (*a*) $k = 5$, $r = 0.9$; (*b*) $k = 5$, $r = 1$; (*c*) magnification of (*b*); (*d*) $k = 20$, $r = 0.95$; (*e*) $k = 20$, $r = 1$; (*f*) magnification of (*e*). For $r = 1$ the approximation (A.4) has been used.

The large n behaviour of the solution of this difference equation is conveniently given by the WKB technique of Dingle and Morgan (1967), based on writing $b_{n+1} + b_{n-1} = 2\cosh\left(\frac{\partial}{\partial n}\right)b_n$ and expressing b_n as the product of a fast-varying exponential and a slowly-varying amplitude. This gives, for the two elementary solutions,

$$b_n \approx \frac{\exp\left\{\pm\int^n \mathrm{d}n' \cosh^{-1} A_{n'}\right\}}{\left(A_n^2 - 1\right)^{1/4}}. \tag{B.3}$$

For large n, approximating ρ_n by (4.6) leads to

$$b_n \approx \left(\frac{\varepsilon n}{4}\right)^{1/4} \exp(\pm 4\sqrt{\varepsilon n}). \tag{B.4}$$

This reveals the profound difference between $\varepsilon = +1$ and $\varepsilon = -1$. With the positive sign, the asymptotic coefficients are growing or decaying exponentials, and imposing the condition

that the growing exponential is absent generates a discrete spectrum in the familiar way. In this case, $\kappa(\phi) \to +\infty$ as $\phi \to 0_{\pm}$, so the negative neighbourhood of the D point, which we previously found to be implicated in the appearance of the continuous spectrum, does not exist.

With the negative sign, the asymptotic coefficients oscillate, and the spectrum appears continuous. In this case, $\kappa(\phi) \to -\infty$ as $\phi \to 0_{\pm}$, so the neighbourhood of the D point is negative on both sides.

Numerical explorations confirm these conclusions, in particular the accuracy of the asymptotic formula (B.4) for both $\varepsilon = +1$ and $\varepsilon = -1$.

References

Abramowitz M and Stegun I A 1972 *Handbook of Mathematical Functions* (Washington: National Bureau of Standards)

Balian R and Bloch C 1970 Distribution of eigenfrequencies for the wave equation in a finite domain: I. Three-dimensional problem with smooth boundary surface *Ann. Phys., NY* **60** 401–47

Baltes H-P and Hilf E R 1976 *Spectra of Finite Systems* (Mannheim: B-I Wissenschaftsverlag)

Berry M V 1981a Quantizing a classically ergodic system: Sinai's billiard and the KKR method *Ann. Phys.* **131** 163–216

Berry M V 1981b Regularity and chaos in classical mechanics, illustrated by three deformations of a circular billiard *Eur. J. Phys.* **2** 91–102

Berry M V 1986 *Quantum Chaos and Statistical Nuclear Physics (Springer Lecture Notes in Physics)* vol 263 ed T H Seligman and H Nishioka pp 1–17

Berry M V 1998 Lop-sided diffraction by absorbing crystals *J. Phys. A: Math. Gen.* **31** 3493–502

Berry M V and Ishio H 2002 Nodal densities of Gaussian random waves satisfying mixed boundary conditions *J. Phys. A: Math. Gen.* 5961–72

Berry M V and Keating J P 1990 A rule for quantizing chaos? *J. Phys. A: Math. Gen.* **23** 4839–49

Born M and Wolf E 2005 *Principles of Optics* (London: Pergamon)

Brown G C, Celli V, Coopersmith M and Haller M 1982 Unitary formalism for scattering from a hard corrugated wall *Phys. Lett.* **90A** 361–3

Dietz B, Eckmann J-P, Pillet C-A, Smilansky U and Ussishkin I 1995 Inside-outside duality for planar billiards: a numerical study *Phys. Rev.* E **51** 4222–31

Dingle R B and Morgan G J 1967 WKB methods for difference equations I *Appl. Sci. Res.* **18** 221–37

Eckmann J-P and Pillet C-A 1995 Spectral duality for planar billiards *Commun. Math. Phys.* **170** 283–313

Gustavson K and Abe T 1998 The third boundary condition—was it Robin's? *Math. Intell.* **20** 63–70

Sieber M, Primack H, Smilansky U, Ussishkin I and Schanz H 1995 Semiclassical quantization of billiards with mixed boundary conditions *J. Phys. A: Math. Gen.* **28** 5041–78

Smilansky U 2004 Irreversible quantum graphs *Waves Random Media* **14** S143–53

Solomyak M 2004 On a differential operator appearing in the theory of irreversible quantum graphs *Waves Random Media* **14** S173–85